Polarization and lattice strains in epitaxial $BaTiO_3$ films grown by high-pressure sputtering

A. Petraru, N. A. Pertsev, H. Kohlstedt, U. Poppe, R. Waser, A. Solbach, and U. Klemradt

Citation: Journal of Applied Physics **101**, 114106 (2007);
View online: https://doi.org/10.1063/1.2745277
View Table of Contents: http://aip.scitation.org/toc/jap/101/11
Published by the American Institute of Physics

Polarization and lattice strains in epitaxial $BaTiO_3$ films grown by high-pressure sputtering

A. Petraru,[a] N. A. Pertsev,[b] H. Kohlstedt, U. Poppe, and R. Waser
Institut für Festkörperforschung and CNI, Forschungszentrum Jülich, D-52425 Jülich, Germany

A. Solbach and U. Klemradt
II. Physikalisches Institut B, RWTH Aachen University, 52074 Aachen, Germany

(Received 5 March 2007; accepted 20 April 2007; published online 14 June 2007)

High-quality $BaTiO_3$ films with thicknesses ranging from 2.9 to 175 nm were grown epitaxially on $SrRuO_3$-covered (001)-oriented $SrTiO_3$ substrates by high-pressure sputtering. The crystal structure of these films was studied by conventional and synchrotron x-ray diffraction. The in-plane and out-of-plane lattice parameters were determined as a function of film thickness by x-ray reciprocal space mapping around the asymmetric $(\bar{1}03)$ Bragg reflection. $BaTiO_3$ films were found to be fully strained by the $SrTiO_3$ substrate up to a thickness of about 30 nm. Ferroelectric capacitors were then fabricated by depositing $SrRuO_3$ top electrodes, and the polarization-voltage hysteresis loops were recorded at the frequencies 1–30 kHz. The observed thickness effect on the lattice parameters and polarization in $BaTiO_3$ films was analyzed in the light of strain and depolarizing-field effects using the nonlinear thermodynamics theory. The theoretical predictions are in reasonable agreement with the measured thickness dependences, although the maximum experimental values of the spontaneous polarization and the out-of-plane lattice parameter exceed the theoretical estimates (43 $\mu C/cm^2$ vs 35 $\mu C/cm^2$ and 4.166 Å vs 4.143 Å). Possible origins of the revealed discrepancy between theory and experiment are discussed. © *2007 American Institute of Physics*.
[DOI: 10.1063/1.2745277]

I. INTRODUCTION

Ferroelectric thin films continue to be the subject of intensive experimental and theoretical research due to their numerous implemented and potential applications in the microelectronics.[1,2] The current trend towards the downscaling of microelectronic devices makes the investigations of size effects on the physical properties of ferroelectric films especially important.

Barium titanate (BTO) is a classical ferroelectric material which was extensively investigated in bulk form in the past.[3] It represents a good choice for experimental studies of the size effects in ferroelectric thin films because detailed comparison between observations and theoretical predictions is possible in this case. In particular, the nonlinear thermodynamics theory of epitaxial ferroelectric films[4,5] can provide quantitative description of BTO films since the thermodynamics parameters of BTO crystals were recently determined with a good degree of precision.[6] This theory describes the influence of substrate-induced lattice strains on the polarization state of an epitaxial film and shows that these strains may induce the formation of new ferroelectric phases in BTO films and increase the spontaneous polarization largely.[4,5] Moreover, several first-principles calculations were performed for ultrathin BTO films.[7–12] The existence of a minimum film thickness for the stability of a single-domain ferroelectric state was predicted, below which it transforms into the paraelectric one owing to the depolarizing-field effect.[8] For $SrRuO_3/BTO/SrRuO_3$ capacitors, the critical thickness of this transformation was found to be reduced markedly by ionic relaxations in the metal-oxide electrodes.[12] The surface effect on ferroelectricity[13] was also confirmed for ultrathin BTO films by the first-principles-based simulations.[10]

The physical properties of BTO films epitaxially grown on various substrates were studied experimentally by several research groups.[14–21] A nonmonotonic variation of the remanent polarization was observed in BTO films grown on $SrTiO_3$ in the range of film thicknesses t between 12 and 80 nm.[14] Extending this study to the thicknesses as small as $t=5$ nm, Kim *et al.* showed that the film polarization strongly decreases in ultrathin films, but even the 5-nm-thick BTO film displays a well-defined polarization hysteresis loop.[18] On the other hand, enormously high remanent polarization $P_r \sim 70$ $\mu C/cm^2$ was found in relatively thick BTO films ($t=200$ nm) grown on $DyScO_3$.[15] This value of P_r is almost 2.7 times higher than the spontaneous polarization $P_s=26$ $\mu C/cm^2$ of bulk BTO (Ref. 22) and about two times larger than the strain-enhanced polarization predicted by the thermodynamics theory for BTO on $DyScO_3$.[23]

For the better understanding of the nature of size effects in ferroelectric films, it is important to measure both the polarization and lattice parameters in a wide range of film thicknesses and to analyze their variations theoretically. In this paper, we report such measurements for BTO films grown by high-pressure sputtering on $SrRuO_3$-covered (001)-oriented $SrTiO_3$ substrates. The growth of epitaxial films and their structural and electrical characterizations is

[a]Electronic mail: a.petraru@fz-juelich.de
[b]On leave from A. F. Ioffe Physico-Technical Institute, Russian Academy of Sciences, 194021 St. Petersburg, Russia; electronic mail: pertsev@domain.ioffe.ru

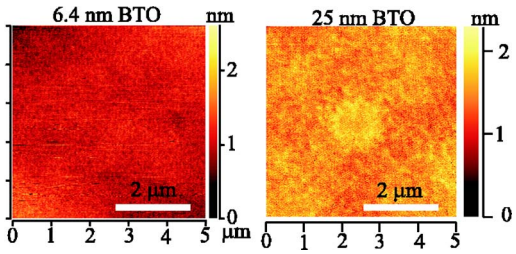

FIG. 1. (Color online) AFM images of the surface of $BaTiO_3$ films grown on $SrRuO_3$-covered $SrTiO_3$ crystals. The film thickness equals 6.4 nm (left image) and 25 nm (right image).

described in Sec. II. The experimental results are summarized in Sec. III, where the thickness dependences of the in-plane lattice strain, out-of-plane lattice parameter, and the film polarization are presented. Section IV describes the theoretical analysis of our experimental data carried out with the aid of the nonlinear thermodynamics theory. Finally, we formulate our conclusions in Sec. V.

II. FILM GROWTH AND CHARACTERIZATION

High-quality epitaxial $SrRuO_3/BaTiO_3/SrRuO_3$ trilayers were deposited by high-pressure sputtering technique[24] on (001)-oriented $SrTiO_3$ (STO) substrates. The surface of commercially obtained substrates was not subjected to chemical treatment and annealing to produce a certain termination. The bottom $SrRuO_3$ (SRO) layer was grown at a substrate temperature of 610 °C and an oxygen pressure inside the sputtering chamber kept at 3 mbars. The BTO films were deposited at 700 °C in a 2.6 mbar pure oxygen atmosphere. These two layers were grown *in situ* with the BTO thickness ranging from 2.9 up to 175 nm. The top SRO layer has been deposited *ex situ* after the x-ray measurements of the BTO one. These measurements were necessary to determine precisely the thickness of each BTO film from the sample series by x-ray diffraction using high-angle finite-size oscillations and low-angle reflectometry.[25] For all samples, the thicknesses of the top and bottom SRO electrodes were about 20 and 80 nm, respectively. The fabricated heterostructures were investigated at room temperature in the as-grown state, no annealing was carried out.

The atomic force microscopy (AFM) measurements showed that the surface of BTO films has a good degree of flatness, with a rms roughness of about 1.9 Å (see Fig. 1). The crystal structure of ferroelectric films was studied by x-ray diffraction experiments performed with the aid of a Philips X'Pert high resolution diffractometer. The $\theta-2\theta$ scans showed that BTO layers are (001) oriented, with the tetragonal c axis orthogonal to the substrate surface. Orientation of the in-plane (100) and (010) crystallographic axes in BTO agrees well with the orientation of the substrate axes, and the films demonstrate a high degree of crystallinity. These features were proved by φ scans of the (101) reflection and ω scans of the (002) reflection of BTO films presented in Fig. 2. The full width at half maximum (FWHM) of the ω scan around the (002) reflection of a 6.4-nm-thick BTO film was 0.028°, which is close to the resolution limit of the instrument.

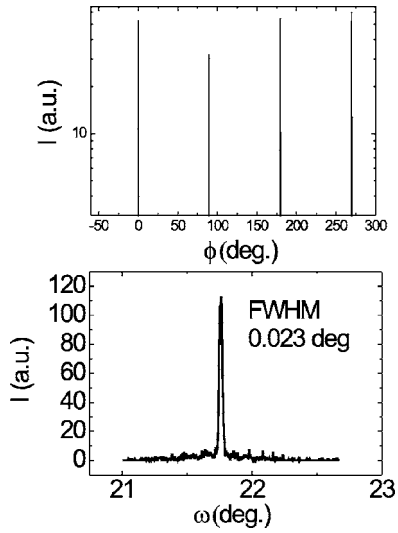

FIG. 2. Φ scan of the (101) reflection and ω scans of the (002) reflection of a 6.4-nm-thick $BaTiO_3$ film.

In order to determine the lattice parameters of BTO films and to evaluate the substrate-induced strains, we performed the x-ray reciprocal space mapping[26] (X-RSM) of our heterostructures around the asymmetric $(\bar{1}03)$ Bragg reflection. Figure 3 shows the maps obtained for BTO films of several different thicknesses. It can be seen that the films are fully strained by the STO substrate up to a thickness of 30 nm. Since the in-plane lattice parameter $a \cong 3.924$ Å of the 56-nm-thick film is considerably larger than the lattice constant $b=3.905$ Å of STO, we infer that the critical thickness t_c for the strain relaxation via the generation of misfit dislocations is about 40 nm. From the X-RSM scans we also extracted the in-plane and out-of-plane lattice parameters of BTO films. Variations of these lattice constants with the film thickness are shown in Fig. 4.

Additional lattice parameter determinations were based on measurements with a Siemens D5000 system and experiments at Hasylab (DESY) using $(\bar{3}03)$ and (002) reflections. The synchrotron radiation data were collected at the high-resolution diffractometer at beamline E2 using a wavelength of 0.78 Å, thus avoiding a background from Sr fluorescence.

For the investigation of the ferroelectric properties of BTO films, plate-capacitor structures were fabricated using optical lithography and Ar^+ ion beam etching. The etching process was monitored with secondary ion mass spectroscopy (SIMS). This enabled us to stop the etching shortly after reaching the surface of BTO layer thus avoiding the damage at the lateral sides of capacitor structures. The fabricated devices had a square shape and the area ranging from 100×100 μm^2 to 4×4 μm^2.

The polarization-voltage hysteresis loops of BTO capacitors were recorded at frequencies 1–30 kHz using an aixACCT TF analyzer 2000. We contacted the electrodes with the aid of micromanipulators and needles. Figure 5 shows typical current-voltage dependences and corresponding polarization-voltage (P-V) loops measured for BTO films of different thicknesses. When the film thickness t is in the range of 25–100 nm, the P-V loop has practically ideal rect-

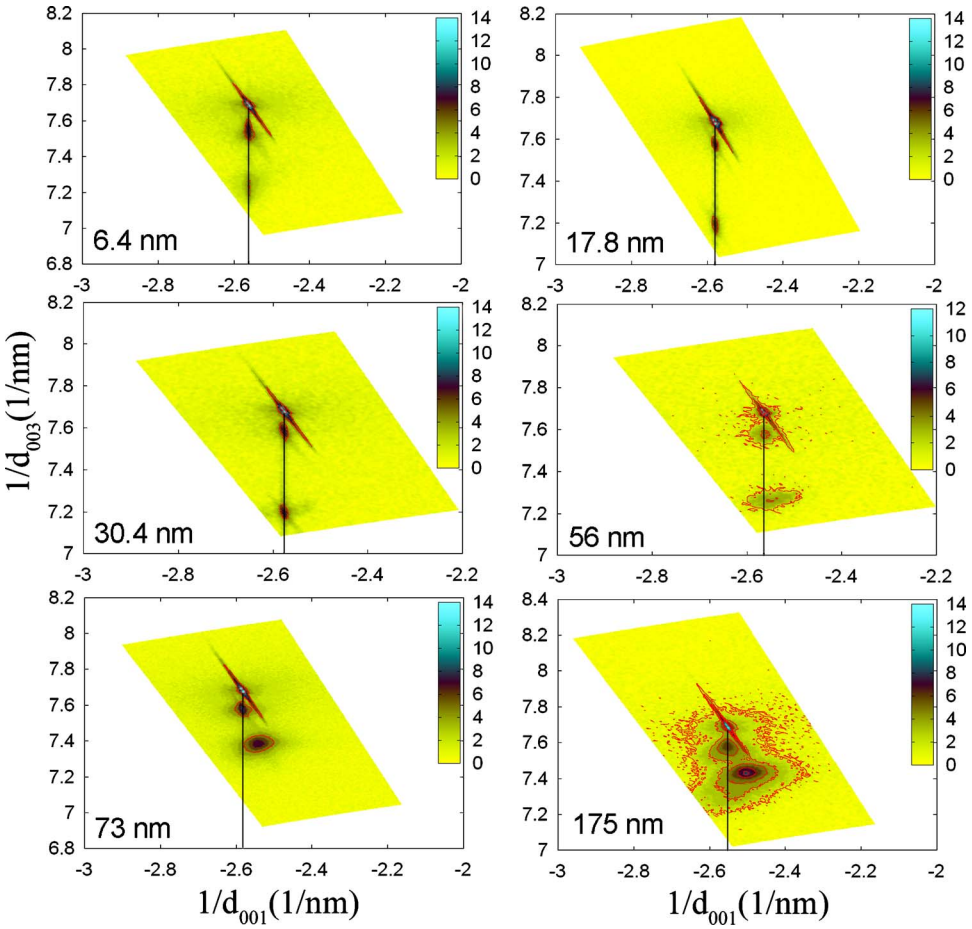

FIG. 3. (Color online) X-ray reciprocal space mapping (X-RSM) around the asymmetric ($\bar{1}03$) Bragg reflection for $BaTiO_3$ films of several different thicknesses.

angular shape [see Fig. 5(a)], which reflects high quality of fabricated BTO films and the absence of nonferroelectric ("dead") layers at the film/electrode interfaces. The loop, however, is shifted from the symmetric position along the voltage axis markedly, which may be attributed to the presence of an internal electric field in the capacitor. At the film thicknesses below 20 nm, the shape of *P-V* loops deteriorates progressively. As can be seen from Fig. 5(b), the hysteresis loop displayed by a 6.4-nm-thick film is compressed along the polarization axis and strongly inclined with respect to this axis. The raw current-voltage curve also demonstrates the presence of a strong leakage current in this film. The leakage current increases further in the thinnest fabricated film ($t=2.9$ nm), but the capacitor is still not short-circuited.

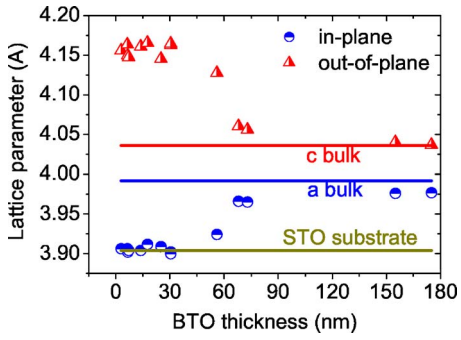

FIG. 4. (Color online) In-plane and out-of-plane lattice parameters of epitaxial $BaTiO_3$ layers plotted as a function of the film thickness.

Although the hysteretic behavior disappears at $t=2.9$ nm [see Fig. 5(c)], the current-voltage dependence remains nonlinear.

III. EXPERIMENTAL RESULTS

The x-ray measurements demonstrate that the lattice parameters of fabricated BTO films differ from those of bulk BTO crystals and vary markedly with the film thickness at $t>t_c\approx 40$ nm (Fig. 4). Hence these epitaxial films have thickness-dependent lattice strains. For the theoretical analysis of the experimental data carried out in Sec. IV, it is necessary to evaluate the misfit strain S_m in our films. This strain can be determined from the measured in-plane lattice parameter a via the relation $S_m=(a-a_0)/a_0$, where a_0 is the lattice parameter of a freestanding film in the prototypic cubic state.[4] Taking a_0 at room temperature to be 4.008 Å (Ref. 5), we obtained the thickness dependence of the misfit strain shown in Fig. 6.

The out-of-plane lattice parameter c decreases with increasing film thicknesses but remains larger than the bulk value of 4.036 Å (Fig. 7). The maximum measured value $c\cong 4.166$ Å exceeds considerably the lattice parameter $c\cong 4.099$ Å observed in BTO films grown on $SrRuO_3/DyScO_3$ at a comparable misfit strain of about -1.7%.[15] On the other hand, enormously large values of the out-of-plane lattice parameter (up to 4.37 Å) were reported by Yanase *et al.* for ultrathin BTO films grown on SRO-covered STO by radio-frequency magnetron sputtering.[14] It should be noted that the lattice parameter c in our films is

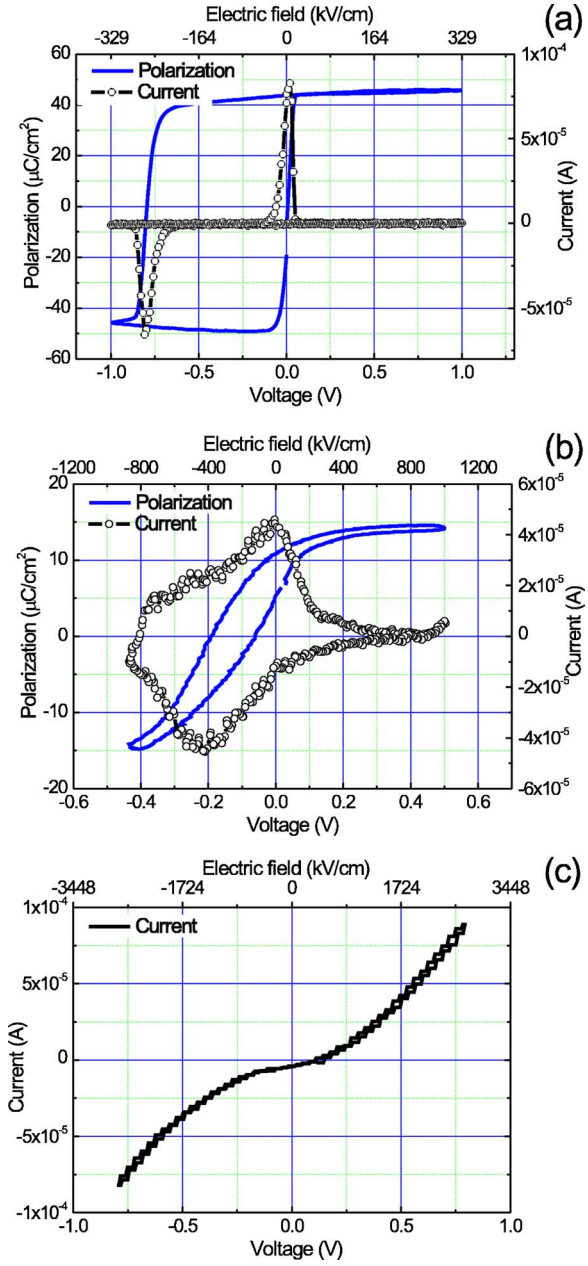

FIG. 5. (Color online) Current-voltage and polarization-voltage characteristics of BTO films sandwiched between SRO electrodes. The film thickness equals 30 nm (a), 6.6 nm (b), and 2.9 nm (c). In the case of the 6.6-nm-thick film, the leakage current was compensated with the aid of the aixACCT TF analyzer 2000.

insensitive to the presence of the top SRO electrode. This feature was demonstrated in a special experiment, in the course of which we compared the values of c measured before and after the deposition of the top electrode.

The hysteretic P-V loops discussed in Sec. II enabled us to determine the film polarization and coercive field. To evaluate the spontaneous polarization P_s, we extrapolated the linear part of $P(V)$ observed at large voltages back to $V=0$. The dependence of thus obtained P_s on the film thickness t is shown in Fig. 8. It can be seen that, with decreasing thickness, the film polarization first gradually increases and then, below $t=25$ nm, starts to drop down. The maximum polarization $P_s \cong 43\ \mu C/cm^2$ observed in our films is close to the

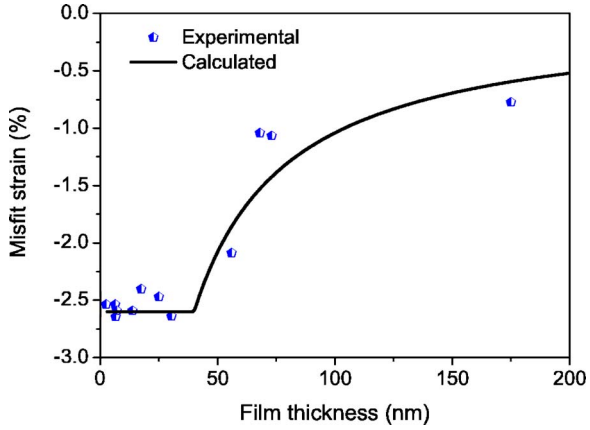

FIG. 6. (Color online) Thickness dependence of the misfit strain in BTO films epitaxially grown on $SrRuO_3$-covered $SrTiO_3$ crystals. Squares show the values obtained from the x-ray measurements, and the solid curve represents the fitting of these values by Eq. (7).

values of 38.5 and 44 $\mu C/cm^2$ reported by Yanase *et al.* and Kim *et al.* for the same heterostructure.[14,18] On the other hand, it is much smaller than the recorded polarization $P_s \cong 70\ \mu C/cm^2$ measured in the 200-nm-thick BTO films grown on $SrRuO_3/DyScO_3$.[15] The thickness dependence of P_s in our films at $t \leqslant 30$ nm is qualitatively similar to the dependence reported in Ref. 18.

Since the P-V loops are shifted from zero voltage (see Fig. 5), the coercive field E_c was evaluated as $E_c=(V_{c2}-V_{c1})/(2t)$, where V_{c2} and V_{c1} are the two measured values of the coercive voltage ($V_{c2}>V_{c1}$). The coercive field was found to be relatively weakly dependent on the film thickness, being about 150 kV/cm. This value is in order-of-magnitude agreement with the coercive fields $E_c=200-300$ kV/cm reported in Ref. 19 for the same heterostructure. At the same time, the coercive fields displayed by epitaxial BTO films are much larger than $E_c \sim 1$ kV/cm characteristic of the bulk crystal.[22] This drastic difference cannot be explained by the strain effect on polarization switching,[27] which is expected to increase E_c by a factor of

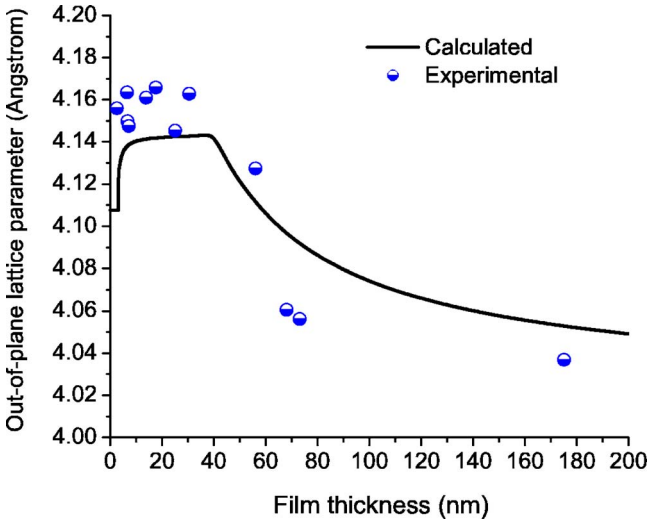

FIG. 7. (Color online) Thickness dependence of the out-of-plane lattice parameter in epitaxial BTO films. Circles show the measured values, and the solid line represents prediction of the thermodynamics theory.

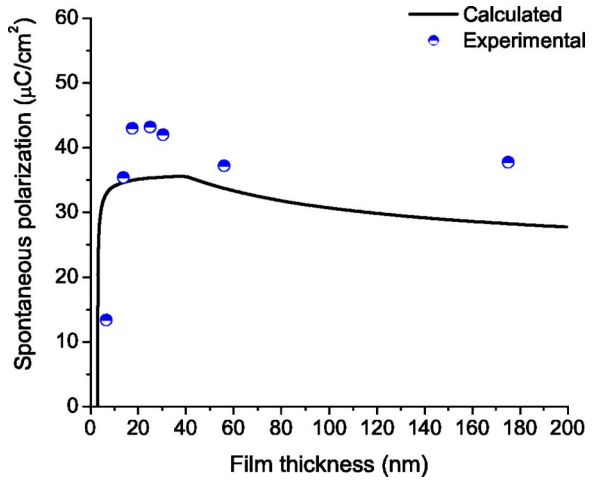

FIG. 8. (Color online) Thickness dependence of the polarization in epitaxial BTO films. Circles show the experimental values, and the solid line represents the theoretical dependence.

$(P_s/P_b)^3 \sim 4$ only (P_b=26 μC/cm^2 is the spontaneous polarization of bulk BTO). It should also be emphasized that strong increase of coercive field at small film thicknesses, which was observed in epitaxial $Pb(Zr_{0.52}Ti_{0.48})O_3$ films sandwiched between SRO and Pt electrodes,[27] is absent in our BTO films. This can be attributed to the absence of nonferroelectric layers at the BTO/SRO interfaces.[19,28] It was shown that the depolarizing field due to the imperfect screening of the polarization charges by the electrodes can become very large, especially in ultrathin film range, and this can produce a backswitching of the polarization via thermally activated nucleation of reverse domains.[28,29]

IV. THEORETICAL ANALYSIS

The observed thickness dependences of the out-of-plane lattice parameter (Fig. 7) and the spontaneous polarization (Fig. 8) are expected to result from the combination of several size effects, including the relaxation of misfit strain in thicker films (Fig. 6), the influence of the depolarizing field,[30] and the intrinsic surface effect on ferroelectricity.[5,13] In this section, we analyze the experimental observations in the light of strain and depolarizing-field effects assuming BTO films to be in a single-domain state.

To describe quantitatively the influence of substrate-induced lattice strains on the orientation and magnitude of the spontaneous polarization, we use the thermodynamics theory of epitaxial ferroelectric films.[4] This theory is based on the polynomial expansion of the energy density in terms of the polarization components P_i $(i=1,2,3)$. Since the eight-order polarization terms in the free energy expansion were found recently to be important for the bulk BTO crystal,[6] we employ the P^8 approximation to calculate the properties of BTO films.

In general, the equilibrium polarization state of an epitaxial ferroelectric film is determined via the minimization of the specific thin-film thermodynamic potential $\tilde{G}$.[4,31] In our case, the Helmholtz free energy density F may be used for this purpose as well since the upper film surface is not subjected to external stresses.[32] The total energy density in a strained film can be written as $F=F_p+F_s+F_c$, where F_p is the energy associated with the ferroelectric polarization, F_s is the elastic strain energy stored in the film, and F_c is the energy of the electrostrictive coupling between polarization and strain. For a ferroelectric with a cubic paraelectric phase, the polarization energy in the P^8 approximation reads

$$\begin{aligned} F_p = {} & a_1(P_1^2+P_2^2+P_3^2)+a_{11}(P_1^4+P_2^4+P_3^4) \\ & +a_{12}(P_1^2P_2^2+P_1^2P_3^2+P_2^2P_3^2)+a_{111}(P_1^6+P_2^6 \\ & +P_3^6)+a_{112}[P_1^4(P_2^2+P_3^2)+P_2^4(P_1^2+P_3^2) \\ & +P_3^4(P_1^2+P_2^2)]+a_{123}P_1^2P_2^2P_3^2+a_{1111}(P_1^8+P_2^8 \\ & +P_3^8)+a_{1112}[P_1^6(P_2^2+P_3^2)+P_2^6(P_1^2+P_3^2) \\ & +P_3^6(P_1^2+P_2^2)]+a_{1122}(P_1^4P_2^4+P_1^4P_3^4 \\ & +P_2^4P_3^4)+a_{1123}(P_1^4P_2^2P_3^2+P_2^4P_1^2P_3^2 \\ & +P_3^4P_1^2P_2^2), \end{aligned} \tag{1}$$

where a_1, a_{ij}, a_{ijk}, and a_{ijkl} are the dielectric stiffness and higher-order dielectric coefficients at constant strain. The strain energy in the harmonic approximation equals

$$\begin{aligned} F_s = {} & \frac{1}{2}c_{11}(S_{11}^2+S_{22}^2+S_{33}^2)+c_{12}(S_{11}S_{22}+S_{11}S_{33}+S_{22}S_{33}) \\ & +2c_{44}(S_{12}^2+S_{13}^2+S_{23}^2), \end{aligned} \tag{2}$$

where c_{mn} are the second-order elastic stiffnesses at constant polarization, and S_{ij} are the lattice strains in the film. The coupling energy may be written as (q_{mn} are the electrostrictive constants)

$$\begin{aligned} F_c = {} & -q_{11}(S_{11}P_1^2+S_{22}P_2^2+S_{33}P_3^2)-q_{12}[S_{11}(P_2^2+P_3^2) \\ & +S_{22}(P_1^2+P_3^2)+S_{33}(P_1^2+P_2^2)]-2q_{44}(S_{12}P_1P_2 \\ & +S_{13}P_1P_3+S_{23}P_2P_3). \end{aligned} \tag{3}$$

The film strains S_{ij} involved in Eqs. (2) and (3) are defined by the mechanical boundary conditions of the problem.[4] For films grown on (001)-oriented cubic substrates, the in-plane film strains S_{11} and S_{22} may be set equal to the misfit strain S_m, whereas the shear strain S_{12} equals zero. The out-of-plane strain S_{33} can be found from the condition $\sigma_{33}=0$ imposed on the stress $\sigma_{33}=\partial F/\partial S_{33}$ in the multilayer with the mechanically free upper surface. This condition yields $S_{33}=[q_{12}(P_1^2+P_2^2)+q_{11}P_3^2-2c_{12}S_m]/c_{11}$. Similarly, the conditions $\sigma_{13}=\sigma_{23}=0$ give us the relations $S_{13}=(q_{44}/2c_{44})P_1P_3$ and $S_{23}=(q_{44}/2c_{44})P_2P_3$ for the shear strains S_{13} and S_{23} in the film. Substitution of the calculated strains into Eqs. (2) and (3) shows that the total film energy F can be written in a form similar to Eq. (1), but with renormalized coefficients of the second- and fourth-order polarization terms. This renormalization of the free energy is described by the formula[32]

$$\begin{aligned} F = {} & \frac{c_{11}^2+c_{11}c_{12}-2c_{12}^2}{c_{11}}S_m^2+a_1^*(P_1^2+P_2^2)+a_3^*P_3^2 \\ & +a_{11}^*(P_1^4+P_2^4)+a_{33}^*P_3^4+a_{12}^*P_1^2P_2^2 \\ & +a_{13}^*(P_1^2+P_2^2)P_3^2+\cdots, \end{aligned} \tag{4}$$

where $a_1^*=a_1-(q_{11}+q_{12}-2q_{12}c_{12}/c_{11})S_m$, $a_3^*=a_1+2S_m(q_{11}c_{12}$

$-q_{12}c_{11})/c_{11}$, $a_{11}^{*}=a_{11}-q_{11}^{2}/(2c_{11})$, $a_{33}^{*}=a_{11}-q_{11}^{2}/(2c_{11})$, $a_{12}^{*}=a_{12}-q_{12}^{2}/c_{11}$, and $a_{13}^{*}=a_{12}-(q_{11}q_{12}/c_{11})-q_{44}^{2}/(2c_{44})$. Using Eq. (4) and performing the minimization of the free energy F with respect to the polarization components P_1, P_2, and P_3, we determined the equilibrium polarization state of a strained BTO film.[33] The calculations showed that in the studied range of misfit strains (Fig. 6) BTO films stabilize at room temperature in the tetragonal c phase with the polarization orthogonal to the surfaces ($P_1=P_2=0$, $P_3\neq 0$). For this phase, the spontaneous polarization $P_s=P_3$ ($V=0$) can be calculated from the relation $\partial F/\partial P_3=0$, which reduces to the following cubic equation for P_S^{2}:

$$a_3^{**}+2a_{33}^{*}P_s^{2}+3a_{111}P_s^{4}+4a_{1111}P_s^{6}=0, \tag{5}$$

where

$$a_3^{**}=a_1+2\frac{(q_{11}c_{12}-q_{12}c_{11})}{c_{11}}S_m+\frac{1}{2c_i t}. \tag{6}$$

As can be seen from Eq. (6), an additional third term was added to the second-order polarization coefficient. This term describes the influence of the depolarizing field, which exists in a ferroelectric capacitor due to imperfect screening of the polarization charges by the electron density variations in the electrodes.[30] Its magnitude is inversely proportional to the film thickness t and the total capacitance c_i of the screening space charge in two electrodes. In our case of SRO electrodes, the "interfacial" capacitance c_i may be set equal to 0.444 $\mathrm{F/m^2}$.[34]

To calculate the film polarization $P_s(t)$, we have to specify the thickness dependence of the misfit strain in Eq. (6) using the data shown in Fig. 6. In the range of small film thicknesses $t\leqslant 40$ nm, the misfit strain may be set equal to the constant value $S_m^0=-2.6\%$.[35] At larger thicknesses, the magnitude of S_m decreases with the film thickness, which may be attributed to the formation of misfit dislocations and progressive increase of their density ρ. Theoretically, the dislocation density should vary with the film thickness as $\rho(t)\cong\eta S_m^0(1-t_c/t)$, where t_c is the critical film thickness and the factor η allows for the partial suppression of the dislocation generation due to kinetic reasons.[36,37] The misfit strain can be evaluated as $S_m\cong[(1-\rho)b-a_0]/a_0$,[38] which gives

$$S_m(t)\cong S_m^0\left[1-\eta\left(1-\frac{t_c}{t}\right)\right]. \tag{7}$$

Equation (7) may be compared with the strain values measured in films with $t>t_c$. As follows from Fig. 6, it is possible to fit the experimental data with a reasonable accuracy by taking $t_c=40$ nm and assuming $\eta=0.9$.

The thickness dependence of spontaneous polarization computed from Eqs. (5)–(7) is shown in Fig. 8. Gradual decrease of P_s with increasing thickness at $t>40$ nm is caused by the strain relaxation, whereas the steep reduction of polarization in ultrathin films is due to the depolarizing-field effect. The size-induced ferroelectric to paraelectric phase transition takes place at $t=2.6$ nm in the single-domain approximation, which is close to the critical thickness of six unit cells predicted by the first-principles calculations for the same heterostructure.[8] However, at a slightly larger thickness of about 3 nm the single-domain state may already become unstable with respect to the formation of a 180° domain structure.[34]

The theoretical dependence $P_s(t)$ is qualitatively similar to the observed polarization variation with the film thickness, but there are two important distinctions between the theory and experiment. First, the maximum measured polarization (about 43 $\mu\mathrm{C/cm^2}$) exceeds the theoretical value $P_S^{\max}\cong 35$ $\mu\mathrm{C/cm^2}$ considerably. Second, the strong decrease of polarization observed in ultrathin films starts at a larger thickness than the theoretically predicted one and proceeds more gradually.

Owing to the electrostriction, any variation of the spontaneous polarization leads to a change of the out-of-plane lattice parameter c. The latter can be calculated from the relation $c=a_0\ (1+S_{33})$, where S_{33} is the lattice strain in the film thickness direction. For the c phase, this relation yields

$$c=a_0\left(1-2\frac{c_{12}}{c_{11}}S_m+\frac{q_{11}}{c_{11}}P_s^{2}\right). \tag{8}$$

Using Eq. (8) and taking into account variations of the misfit strain and spontaneous polarization with the film thickness, we calculated the thickness dependence of the out-of-plane lattice parameter. As can be seen from Fig. 7, the theoretical predictions are again in qualitative agreement with the measurements. Moreover, the maximum value of the measured lattice parameter is only slightly larger than the calculated one (4.166 Å vs 4.143 Å).

One unexplored possibility to improve the accuracy of the thermodynamics theory of epitaxial thin films[4] is to use the nonlinear theory of elasticity to evaluate the strain energy F_s stored in the film.[23] As a first step in this direction, we may add the third-order terms to Eq. (2). For a cubic crystal, the elastic energy in the absence of shear strains can be written as

$$\begin{aligned}F_s=&\frac{1}{2}c_{11}(S_{11}^2+S_{22}^2+S_{33}^2)+c_{12}(S_{11}S_{22}+S_{11}S_{33}+S_{22}S_{33})\\&+\frac{1}{6}c_{111}(S_{11}^3+S_{22}^3+S_{33}^3)+\frac{1}{2}c_{112}[S_{11}^2(S_{22}+S_{33})\\&+S_{22}^2(S_{11}+S_{33})+S_{33}^2(S_{11}+S_{22})]+c_{123}S_{11}S_{22}S_{33},\end{aligned} \tag{9}$$

where c_{lmn} are the third-order elastic constants. The in-plane strains S_{11} and S_{22} here may be set equal to the misfit strain again. The out-of-plane strain S_{33} can be found from the condition $\partial F/\partial S_{33}=0$ using Eq. (9) and retaining Eq. (3) for the coupling energy. For the tetragonal c phase, the calculation gives

$$S_{33} = -\frac{c_{11} + 2c_{112}S_m}{c_{111}} + \sqrt{\frac{(c_{11} + 2c_{112}S_m)^2}{c_{111}^2} + 2\frac{q_{11}P_3{}^2 - 2c_{12}S_m - (c_{112} + c_{123})S_m^2}{c_{111}}}. \tag{10}$$

Substituting this expression back to Eqs. (3) and (9) and summing all contributions to the Helmholtz energy $F=F_p+F_s+F_c$ at $P_1=P_2=0$ and $S_{12}=S_{13}=S_{23}=0$, we obtain an analytic expression for the total energy F of the c phase. The polarization-dependent part of F reads

$$\Delta F = \left(a_1 + \frac{c_{11}q_{11}}{c_{111}} + 2\frac{c_{112}q_{11} - c_{111}q_{12}}{c_{111}}S_m + \frac{1}{2c_i t}\right)P_3{}^2 + a_{11}P_3{}^4 + a_{111}P_3{}^6 + a_{1111}P_3{}^8$$
$$- \frac{1}{3c_{111}^2}\{(c_{11} + 2c_{112}S_m)^2 + 2c_{111}[q_{11}P_3{}^2 - 2c_{12}S_m - (c_{112} + c_{123})S_m^2]\}^{3/2}. \tag{11}$$

As can be seen from Eq. (11), the energy density cannot be cast anymore into a polynomial form characteristic of the polarization energy F_p. In nonlinear elasticity, therefore, the strain effect does not reduce to the renormalization of the dielectric stiffnesses a_1 and a_{ij}. As a result, the equilibrium out-of-plane polarization P_3 can be calculated only numerically from the equation

$$a_1 + \frac{c_{11}q_{11}}{c_{111}} + 2\frac{c_{112}q_{11} - c_{111}q_{12}}{c_{111}}S_m + \frac{1}{2c_i t} + 2a_{11}P_3{}^2 + 3a_{111}P_3{}^4 + 4a_{1111}P_3{}^6$$
$$- \frac{q_{11}}{c_{111}}\sqrt{(c_{11} + 2c_{112}S_m)^2 + 2c_{111}[q_{11}P_3{}^2 - 2c_{12}S_m - (c_{112} + c_{123})S_m^2]} = 0, \tag{12}$$

which follows from the condition $\partial F/\partial P_3=0$.

We employed Eqs. (10) and (12) to analyze the influence of elastic nonlinearity on the out-of-plane lattice parameter and polarization in BTO films fully strained by the STO substrate. Since we were unable to find any data on the third-order elastic constants c_{lmn} of BTO crystals, their values were varied to check whether it is possible to increase the film polarization from 35 to 43 $\mu C/cm^2$ by the nonlinearity of elastic properties. Although such enhancement can be formally achieved, more detailed analysis shows that the measured values of polarization and lattice parameter cannot be fitted simultaneously even by using c_{lmn} as adjustable parameters. This conclusion follows from the general relation $S_{33}=[a_1+1/(2c_it)+2a_{11}P_3{}^2+3a_{111}P_3{}^4+4a_{1111}P_3{}^6-2q_{12}S_m]/q_{11}$ between the out-of-plane strain and the equilibrium polarization, which holds irrespective of the mathematical expression chosen for the elastic energy F_s. It shows that the enhancement of polarization up to 43 $\mu C/cm^2$ is accompanied by an enormous increase of the lattice parameter up to $c=4.40$ Å, which is much larger than the measured value of 4.166 Å. Therefore, the discrepancy between the theoretical and experimental values of the maximum film polarization cannot be attributed to the nonlinearity of the elastic properties of BTO.

V. CONCLUSIONS

Our experimental study confirmed that the polarization and lattice strains in epitaxial BTO films may vary with the film thickness considerably. The out-of-plane lattice parameter of very thin films ($t \leqslant 30$ nm) exceeds the bulk value largely, which can be explained by the influence of biaxial compressive strain induced in the film plane by STO substrate. The maximum measured value of the out-of-plane lattice parameter is very close to the value predicted by the nonlinear thermodynamics theory. In contrast, the maximum measured polarization exceeds the theoretical value significantly (by about 23%). Comparison of the theory with experiment thus reveals qualitatively the same situation as in the case of BTO films grown on $DyScO_3$ and $GdScO_3$.[15] For these films, the temperature dependence of the out-of-plane parameter can be well reproduced by the thermodynamics theory,[15] whereas the measured polarization strongly exceeds the theoretically predicted value (e.g., 70 $\mu C/cm^2$ vs 32 $\mu C/cm^2$ in the case of BTO on $DyScO_3$).

The theoretical analysis presented in Sec. IV demonstrates that the nonlinearity of the elastic properties alone cannot explain the discrepancy between the theory and experiment. Possible increase of electrostrictive constants in strained thin films relative to their bulk values does not represent a reasonable explanation either, because the calculation shows that the polarization depends on these constants rather weakly. In addition, the polarization enhancement caused by the electrostrictive coupling must be larger in BTO films grown on STO than in (less strained) films on $DyScO_3$, which contradicts the experimental data.

Finally, we would like to note that reversible polarization may also increase in BTO films due to the presence of dipolar defects. Indeed, such defects were found to induce low-temperature ferroelectricity in (unstrained) thin films of STO,[39,40] which is an incipient ferroelectric in the bulk form. However, the out-of-plane lattice parameter of these films at room temperature was significantly larger than the bulk lattice constant, probably because the dipolar defects involved oxygen vacancies.[40] Hence it remains unclear whether the defect-induced additional increase of spontaneous polarization could be accompanied by a negligible lattice expansion.

All in all, the origin of the polarization enhancement observed in epitaxial BTO thin films requires further experimental and theoretical investigations.

ACKNOWLEDGMENTS

We thank A. Assmann for help with the x-ray measurements. The financial support of Hasylab through project II-05-079 and the Deutsche Forschungsgemeinschaft under Grant No. KL 1021/4-1 and Volkswagen-Stiftung within the program "Complex Materials: Cooperative Projects of the Natural, Engineering, and Biosciences" under project I/77 737 entitled "Nano-sized ferroelectric Hybrids" is gratefully acknowledged.

[1] O. Auciello, J. F. Scott, and R. Ramesh, Phys. Today **51**(7), 22 (1998).
[2] J. F. Scott, *Ferroelectric Memories* (Springer, Berlin, 2000).
[3] F. Jona and G. Shirane, *Ferroelectric Crystals* (Macmillan, New York, 1962).
[4] N. A. Pertsev, A. G. Zembilgotov, and A. K. Tagantsev, Phys. Rev. Lett. **80**, 1988 (1998); Ferroelectrics **223**, 79 (1999).
[5] A. G. Zembilgotov, N. A. Pertsev, H. Kohlstedt, and R. Waser, J. Appl. Phys. **91**, 2247 (2002).
[6] Y. L. Li, L. E. Cross, and L. Q. Chen, J. Appl. Phys. **98**, 064101 (2005).
[7] S. Tinte and M. G. Stachiotti, Phys. Rev. B **64**, 235403 (2001).
[8] J. Junquera and Ph. Ghosez, Nature (London) **422**, 506 (2003).
[9] O. Diéguez, S. Tinte, A. Antons, C. Bungaro, J. B. Neaton, K. M. Rabe, and D. Vanderbilt, Phys. Rev. B **69**, 212101 (2004).
[10] B.-K. Lai, I. A. Kornev, L. Bellaiche, and G. J. Salamo, Appl. Phys. Lett. **86**, 132904 (2005).
[11] N. Sai, A. M. Kolpak, and A. M. Rappe, Phys. Rev. B **72**, 020101(R) (2005).
[12] G. Gerra, A. K. Tagantsev, N. Setter, and K. Parlinski, Phys. Rev. Lett. **96**, 107603 (2006).
[13] R. Kretschmer and K. Binder, Phys. Rev. B **20**, 1065 (1979).
[14] N. Yanase, K. Abe, N. Fukushima, and T. Kawakubo, Jpn. J. Appl. Phys., Part 1 **38**, 5305 (1999).
[15] K. J. Choi *et al.*, Science **306**, 1005 (2004).
[16] D. A. Tenne *et al.*, Phys. Rev. B **69**, 174101 (2004).
[17] O. Trithaveesak, J. Schubert, and Ch. Buchal, J. Appl. Phys. **98**, 114101 (2005).
[18] D. J. Kim, J. Y. Jo, Y. S. Kim, Y. J. Chang, J. S. Lee, J.-G. Yoon, T. K. Song, and T. W. Noh, Phys. Rev. Lett. **95**, 237602 (2005).
[19] Y. S. Kim *et al.*, Appl. Phys. Lett. **88**, 072909 (2006).
[20] F. He and B. O. Wells, Appl. Phys. Lett. **88**, 152908 (2006).
[21] B. Dkhil, E. Defay, and J. Guillan, Appl. Phys. Lett. **90**, 022908 (2007).
[22] B. Jaffe, W. R. Cook, Jr., and H. Jaffe, *Piezoelectric Ceramics* (Academic, London, 1971).
[23] N. A. Pertsev, Mater. Res. Soc. Symp. Proc. **902E**, (2006).
[24] U. Poppe *et al.*, Solid State Commun. **66**, 661 (1988).
[25] J.-M. Triscone, P. Fivat, M. Andersson, M. Decroux, and Ø. Fisher, Phys. Rev. B **50**, 1229 (1994).
[26] U. Pietsch, V. Holý, and T. Baumbach, *High-Resolution X-Ray Scattering*, 2nd ed. (Springer, Berlin, 2004), Chap. 9.
[27] N. A. Pertsev, J. Rodriguez Contreras, V. G. Kukhar, B. Hermanns, H. Kohlstedt, and R. Waser, Appl. Phys. Lett. **83**, 3356 (2003).
[28] J. Y. Jo, Y. S. Kim, T. W. Noh, J.-G. Yoon, and T. K. Song, Appl. Phys. Lett. **89**, 232909 (2006).
[29] J. Y. Jo, D. J. Kim, Y. S. Kim, S.-B. Choe, T. K. Song, J.-G. Yoon, and T. W. Noh, Phys. Rev. Lett. **97**, 247602 (2006).
[30] R. R. Mehta, B. D. Silverman, and J. T. Jacobs, J. Appl. Phys. **44**, 3379 (1973).
[31] A. Yu. Emelyanov, N. A. Pertsev, and A. L. Kholkin, Phys. Rev. B **66**, 214108 (2002).
[32] N. A. Pertsev, A. K. Tagantsev, and N. Setter, Phys. Rev. B **61**, R825 (2000).
[33] In the numerical calculations, we used the following set of thermodynamic parameters and material constants of BTO crystals (in SI units): $a_1=4.124(T-115)\times10^5$, $a_{11}=5.328\times10^8$, $a_{12}=3.426\times10^8$, $a_{111}=1.294\times10^9$, $a_{112}=-1.95\times10^9$, $a_{123}=-2.5\times10^9$, $a_{1111}=3.863\times10^{10}$, $a_{1112}=2.529\times10^{10}$, $a_{1122}=1.637\times10^{10}$, $a_{1123}=1.367\times10^{10}$, $c_{11}=1.755\times10^{11}$, $c_{12}=8.464\times10^{10}$, $c_{44}=1.082\times10^{11}$, $q_{11}=1.203\times10^{10}$, $q_{12}=-1.878\times10^9$, and $q_{44}=6.385\times10^9$. This set corresponds to the thermodynamics parameters of BTO reported in Ref. 6 and the electrostrictive and elastic constants listed in Ref. 4.
[34] N. A. Pertsev and H. Kohlstedt, e-print cond-mat/0603762 <http://arxiv.org/abs/cond-mat/0603762v2> [cond-mat.mtrl-sci].
[35] This value is equal to the nominal misfit strain $S_m^0=(b-a_0)/a_0$ between BTO and STO (b is the lattice parameter of the substrate).
[36] J. Matthews and A. E. Blakeslee, J. Cryst. Growth **27**, 118 (1974).
[37] R. Dittmann, R. Plonka, E. Vasco, N. A. Pertsev, J. Q. He, C. L. Jia, S. Hoffmann-Eifert, and R. Waser, Appl. Phys. Lett. **83**, 5011 (2003).
[38] J. S. Speck and W. Pompe, J. Appl. Phys. **76**, 466 (1994).
[39] D. Fuchs, C. W. Schneider, R. Schneider, and H. Rietschel, J. Appl. Phys. **85**, 7362 (1999).
[40] D. Fuchs, M. Adam, P. Schweiss, S. Gerhold, S. Schuppler, R. Schneider, and B. Obst, J. Appl. Phys. **88**, 1844 (2000).